Results for Heavy Flavor and Quarkonium production in high multiplicity p+p and p+A collisions in the CGC framework

Kazuhiro Watanabe

Old Dominion Univ / Jefferson Lab

April 19, 2018
DIS2018 at Kobe

with Y.-Q. Ma (Peking U), P. Tribedy (BNL), R. Venugopalan (BNL)
arXiv:1803.11093

High multiplicity events

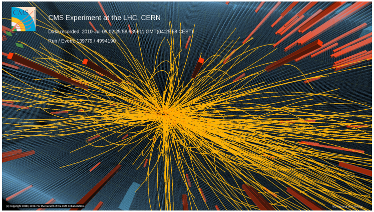

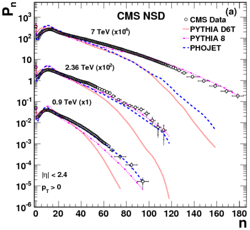

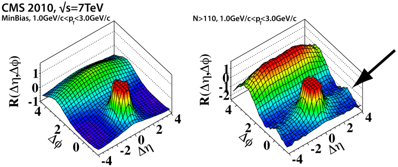

- Discovery of ridge like structure: the starting point.
- p+p vs p+A vs A+A: Initial state (fluctuation) or Final state (hydro) origins?
- Interplay of hard and soft collisions.
- Gluon saturation is a natural way to explain this phenomenon. cf. [Dumitru et al. (2010)]

Motivation

Gluon saturation describes systematically heavy flavor and onium production in high multiplicity p+p and p+A collisions ?

Gluon saturation and high multiplicity

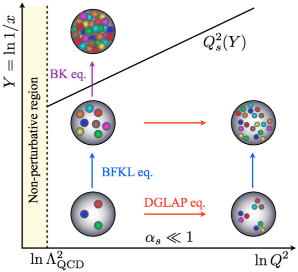

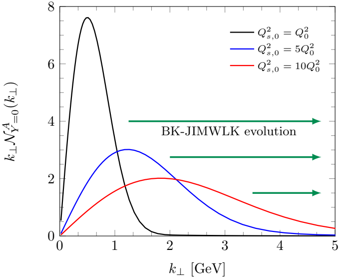

- Gluon recombination at small-x → Glauon Saturation

$$Q^2_{s,A} \propto \# \frac{\alpha_s}{S_{A\perp}} x G_A \sim \# A^{1/3} \left(\frac{1}{x}\right)^{\lambda} \sim \# A^{1/3} Q^2_{s,p}$$

✓ $k_\perp > Q_s$: Gluons are hard, pQCD is applicable.
✓ $k_\perp < Q_s$: Gluons are soft and high occupied in "Saturation region".

- High multiplicity events: Spacial and momentum structure of rare parton configurations are important.
⟹ Such rare parton configurations can be controlled by $Q_s(x)$. cf. [Dusling, Venugopalan (2012)]

Large Q_s (hadron fluctuation) ↔ Soft gluon modes are enhanced ↔ High multiplicity

Why heavy quark?

- ✓ Heavy flavor and Onium are complementary observables to light hadron, dijet production. → Event engineering studies.
- ✓ Provides unique playground to study gluon saturation or test the CGC framework. Remind $c\bar{c}$ is largely produced via initial gluon fusion at collider energies.
- ✓ Saturation scales are semihard at the energy frontier: m_c vs $Q_{sp}(x_1)$ vs $Q_{sA}(x_2)$
- ✓ The CGC can be helpful in understanding of heavy flavor and onium production mechanisms at low-$p_\perp$.

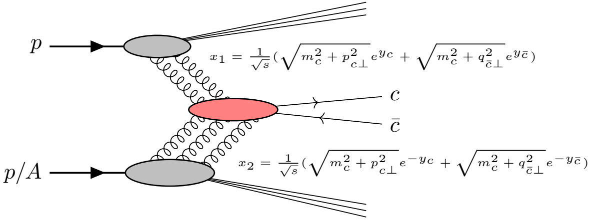

The Color-Glass-Condensate (CGC) framework

- projectile moving $\rightarrow x^+ = +\infty$, target moving $\rightarrow x^- = +\infty$.
- Solving classical Yang-Mills eq. : $[D^\mu, F_{\mu\nu}] = J^\nu \Longrightarrow |\mathcal{T}\rangle = \sum_i^\infty |\underbrace{gg\cdots gg}_{i}\rangle$

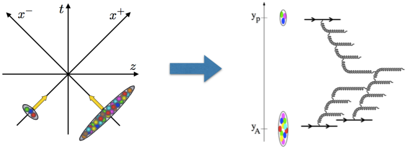

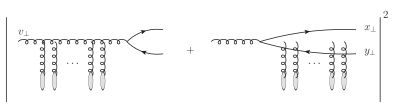

[Blaizot, Gelis, Venugopalan (2004)]

$$\frac{d\sigma_{c\bar{c}}}{d^2\boldsymbol{p}_{c\perp} d^2\boldsymbol{q}_{\bar{c}\perp} dy_c dy_{\bar{c}}} = \frac{\alpha_s N_c^2 \pi R_A^2}{2(2\pi)^{10} d_A} \int_{\boldsymbol{k}_{2\perp},\boldsymbol{k}_\perp} \frac{\varphi_{p,y_p}(\boldsymbol{k}_{1\perp})}{k_{1\perp}^2} \mathcal{N}_Y(\boldsymbol{k}_\perp)\mathcal{N}_Y(\boldsymbol{k}_{2\perp} - \boldsymbol{k}_\perp)\, \Xi$$

- Unintegrated gluon distribution function: $\varphi_{p,y_p}(\boldsymbol{k}_\perp) = \pi R_p^2 \frac{N_c k_\perp^2}{4\alpha_s} \mathcal{N}_{y_p}^A(\boldsymbol{k}_\perp)$
- Dipole amplitude: $\mathcal{N}_{y_p(Y)}(\boldsymbol{k}_\perp) = \int d^2\boldsymbol{r}_\perp e^{-i\boldsymbol{k}_\perp\cdot\boldsymbol{r}_\perp} \frac{1}{N_c} \left\langle \mathrm{Tr}\left[V_F(\boldsymbol{r}_\perp)V_F^\dagger(\boldsymbol{0}_\perp)\right]\right\rangle_{y_p(Y)}$
- The rcBK equation descries x-evolution of the dipole amplitude. $(\mathcal{N}_Y(\boldsymbol{k}_\perp) = F.T.\ of\ D_Y(\boldsymbol{r}_\perp))$ [Balitsky (2006)]

$$-\frac{dD_{Y,\boldsymbol{r}_\perp}}{dY} = \int d^2\boldsymbol{r}_{1\perp} \mathcal{K}(r_\perp, r_{1\perp})\left[D_{Y,\boldsymbol{r}_\perp} - D_{Y,\boldsymbol{r}_{1\perp}} D_{Y,\boldsymbol{r}_{2\perp}}\right]$$

1. Minimum Bias events
   - D meson production
   - J/ψ production
   - $\psi(2S)$ production
   - Υ production

2. High multiplicity events
   - D meson production vs N_{ch}
   - J/ψ meson production vs N_{ch}

A quick guide to numerical calculations

- $m = 1.3$ GeV for D meson and J/ψ. But $m = 1.5$ GeV $\approx m_{J/\psi}/2$ is used only when NRQCD factorization is employed.
- α_s is fixed.
- Initial saturation scale of proton: $Q^2_{sp,0} = Q^2_0 = 0.168$ GeV at $x = 0.01$. $\Longleftarrow$ HERA-DIS global data fitting. [AAMQS (2010)]

$$D_{Y=Y_0,\boldsymbol{r}_\perp} = \exp\left[-\frac{\left(r_\perp^2 Q^2_{sp,0}\right)^\gamma}{4}\ln\left(\frac{1}{r_\perp\Lambda}+e\right)\right],$$

- Initial saturation scale of nucleus: $Q^2_{sA,0} = 2Q^2_0$. $\Longleftarrow$ A fit to the available NMC (New Muon Collab.) data (fixed target eA) on the nuclear structure functions $F_{2,A}(x, Q^2)$ at $x \sim 0.01$. [Dusling, Gelis, Lappi, Venugopalan (2009)]
- φ at large-x: Matching between φ and collinear PDF xG with CTEQ6M set at $x = 0.01$.

$$\mathcal{N}^A_Y(\boldsymbol{k}_\perp) \overset{x>x_0}{=} \frac{xG_{\mathrm{CTEQ}}(x, Q_0^2)}{xG^{\mathrm{Dipole}}(x_0, Q_0^2)}\mathcal{N}^A_{Y_0}(\boldsymbol{k}_\perp)$$

with the identity $xG^{\mathrm{Dipole}}(x, Q_0^2) = \frac{1}{4\pi^3}\int_0^{Q_0^2} dk_\perp^2 \varphi_Y(k_\perp)$. Switch from φ to xG at $x > x_0$.

- $R_p \sim 0.5$ fm, $Q_0 \sim 5$ GeV are obtained from the matching. R_A is chosen to reproduce $R_{pA} = \frac{d\sigma_{pA}}{A d\sigma_{pp}} = 1$ when $p_\perp \to \infty$.

D meson production

[Fujii, KW (2013)][Ma, Tribedy, Venugopalan, KW (2018)]

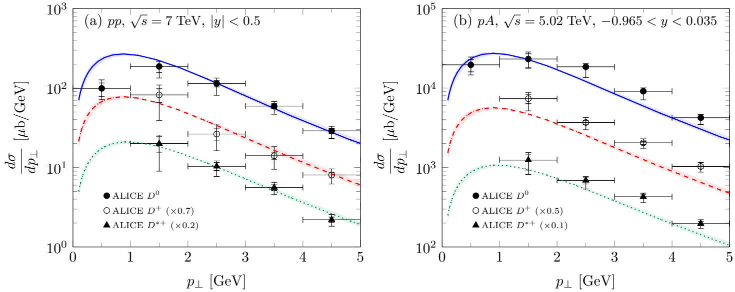

$$\frac{d\sigma_D}{d^2\boldsymbol{p}_{D\perp}dy} = \int_{z_{min}}^{1} dz \frac{D_{c\to D}(z)}{z^2} \int dy_{\bar{c}} \int_{\boldsymbol{q}_{\bar{c}\perp}} \frac{d\sigma_{c\bar{c}}}{d^2\boldsymbol{p}_{c\perp}d^2\boldsymbol{q}_{\bar{c}\perp}dy\,dy_{\bar{c}}}$$

- $D_{c\to D}(z)$: BCFY Fragmentation Function [Braaten, Cheung, Fleming, Yuan(1994)]

[Ma, Venugopalan (2014)][Ma, Venugopalan, Zhang (2015)]

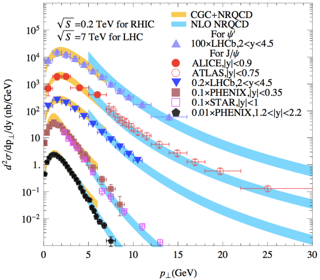

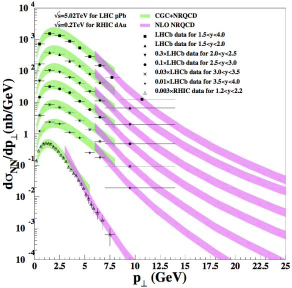

- The CGC cross sections at short distance are matched to NRQCD LDMEs.

$$\frac{d\sigma^{\psi}}{dy\,dp_\perp^2} = \sum_{\kappa} \underbrace{\frac{d\hat{\sigma}^{\kappa}_{c\bar{c}}}{dy\,dp_\perp^2}}_{\text{CGC}} \times \underbrace{\left\langle O^{\psi}_{\kappa} \right\rangle}_{\text{LDMEs}} \qquad (\kappa = {}^{2S+1}L_J^{[c]})$$

- The LDMEs are extracted from high $p_\perp$ data fitting at Tevatron. [Chao et al. (2012)]

$$\langle O^{J/\psi}[{}^1S_0^{[8]}]\rangle = 0.089 \pm 0.0098\text{GeV}^3,\ \langle O^{J/\psi}[{}^3S_1^{[8]}]\rangle = 0.0030 \pm 0.0012\text{GeV}^3,$$
$$\langle O^{J/\psi}[{}^3P_0^{[8]}]\rangle = 0.0056 \pm 0.0021\text{GeV}^3$$

- The contribution of CS channel is relatively small. (10% in pp, 15% – 20% in pA at small-$p_\perp$)

J/ψ production in the CGC + Improved CEM

- Color Evaporation Model (CEM) is consistent with NRQCD in the sense that color octet $c\bar{c}$ is mainly considered.
- Improved CEM (ICEM) can reproduce different $p_\perp$ distributions of J/ψ and $\psi(2S)$ correctly. [Ma, Vogt (2016)]

$$\frac{d\sigma_\psi}{d^2p_\perp dy} = F_{c\bar{c}\to\psi}\int_{m_\psi}^{2m_D} dM \left(\frac{M}{m_\psi}\right)^2 \frac{d\sigma_{c\bar{c}}}{dM\,d^2p'_\perp dy}\bigg|_{p'_\perp=\frac{M}{m_\psi}p_\perp}$$

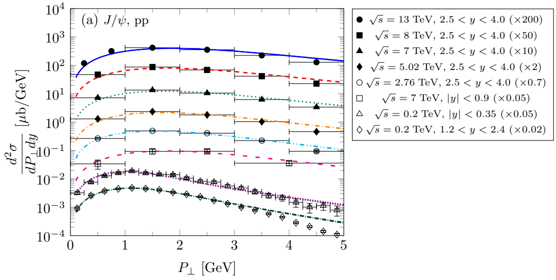

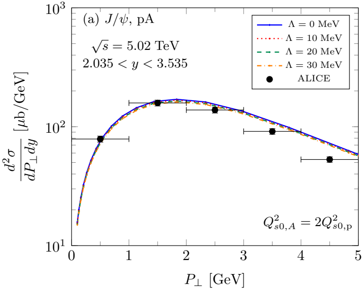

[Ma, Venugopalan, Zhang, KW (2017)]

$\psi(2S)$ production

- Soft color exchanges between partonic comovers and the $c\bar{c}$ can affect greatly $\psi(2S)$ production. [Ma, Venugopalan, Zhang, KW (2017)]

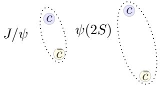

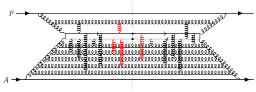

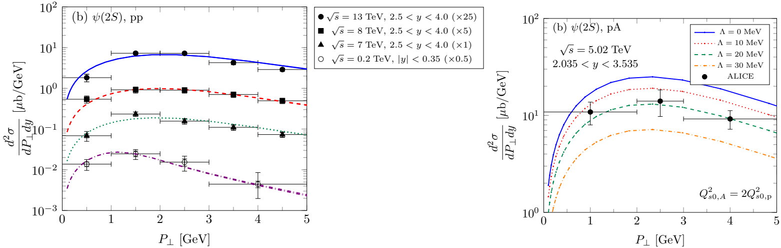

- In p+p collisions, $F_{q\bar{q}\to\psi}$ is fitted and should include the effect of soft color exchanges at final stage.
- Important assumption : the role of soft color exchanges should be enhanced in p+A collisions. $\rightarrow$ Λ is responsible for the nuclear enhancement effect.

$$\frac{d\sigma_\psi}{d^2p_\perp dy} = F_{c\bar{c}\to\psi} \int_{m_\psi}^{2m_D-\Lambda} dM \left(\frac{M}{m_\psi}\right)^2 \frac{d\sigma_{c\bar{c}}}{dM\, d^2p'_\perp dy}\bigg|_{p'_\perp = \frac{M}{m_\psi}p_\perp}$$

where Λ denotes the average momentum kick given by additional nuclear parton comovers.

$\Upsilon(1S)$ production

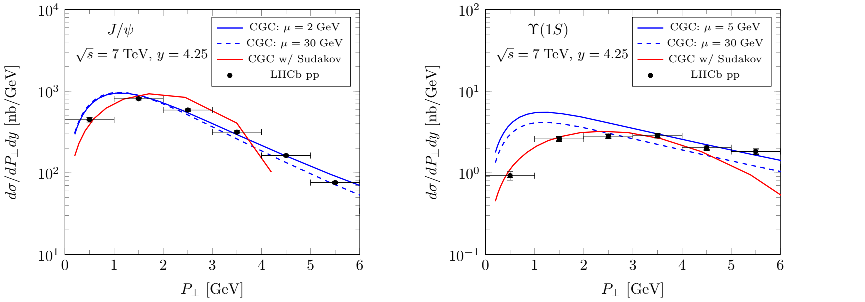

- Large Mass scale $\rightarrow \#\alpha_s \ln^2 \dfrac{M^2}{p_\perp^2} \sim \mathcal{O}(1)$. (Sudakov double logs)
- The soft gluon shower effect and the saturation effect can be described straightforwardly in the hybrid framework: [K.W., Xiao (2015)]

$$d\sigma^{c\bar{c}}_{\text{resum}} \propto \int \frac{d^2u_\perp d^2v_\perp}{(2\pi)^4}\, e^{-ip_{\text{rel}}\cdot u_\perp} e^{ip_\perp\cdot v_\perp} x_1 G\Big(x_1, \frac{c_0}{v_\perp}\Big) D_Y(x_\perp) D_Y(y_\perp) e^{-S_{\text{Sud}}(M, v_\perp)} \hat{H}_{\text{LO}},$$

with $x_\perp = v_\perp + (1-z)u_\perp$ and $y_\perp = v_\perp - zu_\perp$.

- S_{Sud} must be "Universal". cf. [Sun, Yuan, Yuan (2012)]
- Sudakov effect is dominant for low-$p_\perp$ Υ production in p+p collisions. cf. [Qiu, K.W. (2017)]
- In p+A collisions, Saturation effect can be comparable to Sudakov effect.

1 Minimum Bias events

- D meson production
- J/ψ production
- $\psi(2S)$ production
- Υ production

2 High multiplicity events

- D meson production vs N_{ch}
- J/ψ meson production vs N_{ch}

Caveats

- Matching between φ_p and xG is no more justified. In lieu, the adopt the simple extrapolation ansatz for φ: [Gelis, Stasto, Venugopalan (2006)]

$$\varphi_{p,y_p}(\boldsymbol{k}_\perp) = \varphi_{p,y_0}(\boldsymbol{k}_\perp)\left(\frac{1-x}{1-x_0}\right)^4 \left(\frac{x_0}{x}\right)^{0.15} .$$

- Hadronization of charm to D meson, J/ψ production models are the same as used in MB events.
- All the input parameters are taken to be the same, except for Q_s.

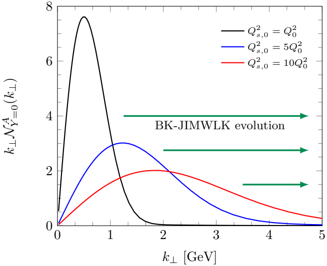

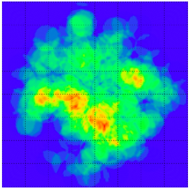

Charged hadron multiplicity in the CGC framework

- $p + p/A \to g(\to h) + X$: [Kovchegov, Tuchin (2001)]

$$\frac{d\sigma_g}{d^2\boldsymbol{p}_{g\perp}dy} = \frac{\alpha_s \hat{K}_b}{(2\pi)^3\pi^3 C_F}\frac{1}{p_{g\perp}^2}\int d^2\boldsymbol{k}_\perp \varphi_{p,y_p}(\boldsymbol{k}_\perp)\,\varphi_{A,Y}(\boldsymbol{p}_{g\perp}-\boldsymbol{k}_\perp)$$

$$\frac{dN_{ch}}{d\eta} = \frac{\hat{K}_{ch}}{\sigma_{\rm inel}}\int d^2\boldsymbol{p}_\perp \int_{z_{\rm min}}^{1} dz\,\frac{D_h(z)}{z^2} J_{y\to\eta}\frac{d\sigma_g}{d^2\boldsymbol{p}_{g\perp}dy}$$

where $J_{y\to\eta} = p_{g\perp}\cosh\eta/\sqrt{p_{g\perp}^2\cosh^2\eta + m_h^2}$ and $\boldsymbol{p}_\perp \equiv z\boldsymbol{p}_{g\perp}$.

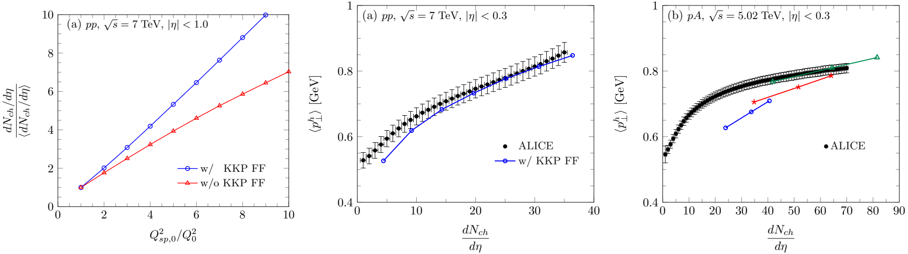

It is clear that the relative N_{ch} grows almost linearly as $Q^2_{sp,0}$ increases when the KKP FF is used.

D meson production vs N_{ch}

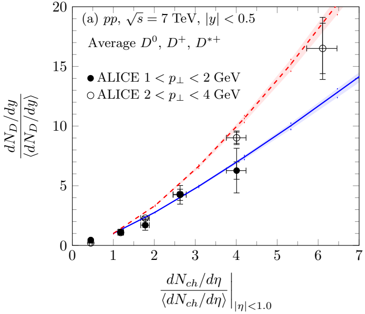

← p+p collisions

- Normalized in MB p+p collisions.

× $Q^2_{sp,proj} > Q^2_0$ and $Q^2_{sp,targ} = Q^2_0$.

× $Q^2_{sp,targ} > Q^2_0$ and $Q^2_{sp,proj} = Q^2_0$.

✓ $Q^2_{sp_1} = Q^2_{sp_2} > Q^2_0$.

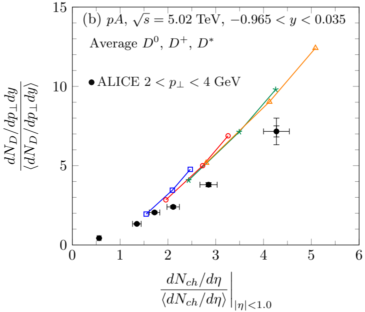

← p+A collisions

- Normalized in MB p+A collisions.
- Different colors: Different $Q^2_{sA,0}$ ⇒ Fluctuation effect of proton is important to achieve high N_{ch} when $Q^2_{sA,0}$ is being fixed.
- The same qualitative trend in p+p and p+A collisions.

J/ψ meson production vs N_{ch} at mid rapidity

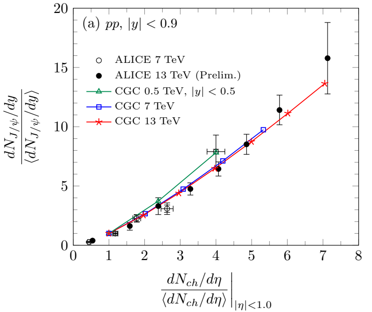

← p+p collisions

- The CGC+ICEM framework is used.
- The ratios are $\sqrt{s}$-independent! In the CGC, events at different energies with the same Q_s are identical.

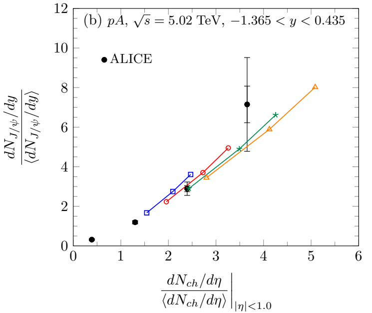

← p+A collisions

- Different colors: Different $Q^2_{sA,0}$

The similar trends are seen for D meson and J/ψ production. → Hadronization dynamics is irrelevant, rather saturation effect at short distance plays a key role in describing data.

J/ψ meson production vs N_{ch} at forward rapidity

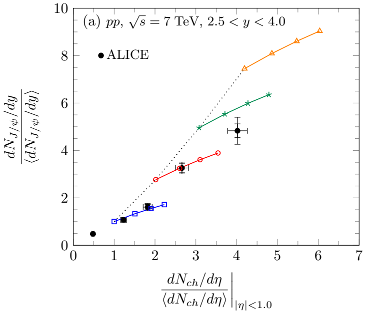

$\leftarrow$ p+p collisions

- Different colors: Different $Q^2_{sp1,0}$ and $Q^2_{sp2,0} \geq Q^2_{sp1,0}$.
- In contrast to mid rapidity, the symmetrical treatment; $Q^2_{sp_1,0} = Q^2_{sp_2,0}$ overshoots the data slightly in $p + p$ collisions (Dashed line). Data point at $dN_{ch} / \langle dN_{ch} \rangle \sim 4$ seems to favor the asymmetrical treatment; $Q^2_{sp_1,0} < Q^2_{sp_2,0}$.

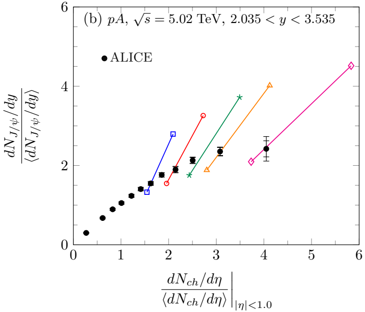

$\leftarrow$ p+A collisions

- Different colors: Different $Q^2_{sA,0}$.
- Lower points: $Q^2_{sp,0} = Q^2_0$, Upper points: $Q^2_{sp,0} = 2Q^2_0$.

N_{ch} dependence of J/ψ production in the CGC+NRQCD

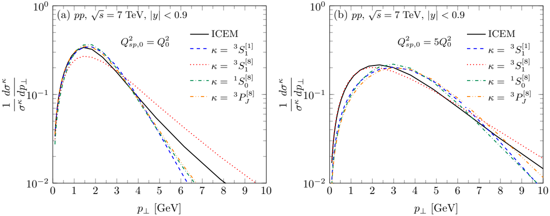

- The normalized $c\bar{c}$ differential cross section for the ${}^3S_1^{[8]}$ channel is close to that of the ICEM over the entire $p_\perp$ range at large $Q^2_{sp,0}$.

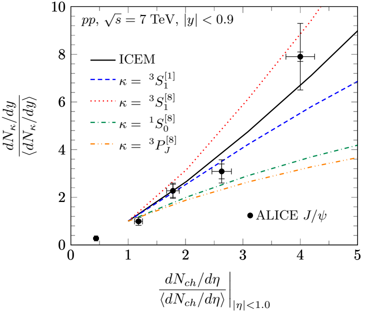

- With increasing event activity, the ${}^3S_1^{[8]}$ state dominates J/ψ production.
- This is remarkably consistent with the universality requirement from BELLE e^+e^- data:

$$\langle \mathcal{O}^{J/\psi}[{}^1S_0^{[8]}]\rangle + 4.0\langle \mathcal{O}^{J/\psi}[{}^3P_0^{[8]}]\rangle/m^2 < 2.0 \pm 0.6 \times 10^{-2}\,\mathrm{GeV}^3$$

[Zhang, Ma, Wang, Chao (2009)]

- Note: the LDMEs used in the CGC+NRQCD previously violates this upper bound.

Summary

- Event engineered Heavy flavor and Onium production in high multiplicity p+p and p+A collisions provide unique opportunity to study gluon saturation phenomenon.
- Excellent agreement is found between the CGC computations and the LHC heavy flavor data on D and J/ψ production in high multiplicity events in p+p and p+A collisions.
- Data comparisons using the CGC+NRQCD framework potentially can distinguish between intermediate states with differing quantum numbers that contribute to the hadronization of J/ψ mesons.

Thank you!

3 Backup

The CGC+NRQCD

[Kang, Ma, Venugopalan (2013)]

$$\frac{d\sigma^{\kappa}_{c\bar{c},\mathrm{CS}}}{d^2\boldsymbol{p}_\perp dy} = \frac{\alpha_s \pi R_A^2}{(2\pi)^9 d_A} \int_{\boldsymbol{k}_{2\perp},\boldsymbol{k}_\perp,\boldsymbol{k}'_\perp} \frac{\varphi_{p,y_p}(\boldsymbol{k}_{1\perp})}{k_{1\perp}^2} \mathcal{N}_Y(\boldsymbol{k}_\perp)\mathcal{N}_Y(\boldsymbol{k}'_\perp)\mathcal{N}_Y(\boldsymbol{k}_{2\perp} - \boldsymbol{k}_\perp - \boldsymbol{k}'_\perp)\ \mathcal{G}_1^{\kappa}$$

$$\frac{d\sigma^{\kappa}_{c\bar{c},\mathrm{CO}}}{d^2\boldsymbol{p}_\perp dy} = \frac{\alpha_s \pi R_A^2}{(2\pi)^7 d_A} \int_{\boldsymbol{k}_{2\perp},\boldsymbol{k}_\perp} \frac{\varphi_{p,y_p}(\boldsymbol{k}_{1\perp})}{k_{1\perp}^2} \mathcal{N}_Y(\boldsymbol{k}_\perp)\mathcal{N}_Y(\boldsymbol{k}_{2\perp} - \boldsymbol{k}_\perp)\ \Gamma_8^{\kappa}$$

BCFY FF

We follow [Cacciari et al. (2012)]:

$$D_{c\to D^0}(z;r) = 0.168 D^{(P)}_{\mathrm{BCFY}}(z;r) + 0.39 \tilde{D}^{(V)}_{\mathrm{BCFY}}(z;r),$$
$$D_{c\to D^+}(z;r) = 0.162 D^{(P)}_{\mathrm{BCFY}}(z;r) + 0.07153 \tilde{D}^{(V)}_{\mathrm{BCFY}}(z;r),$$
$$D_{c\to D^*}(z;r) = 0.233 D^{(V)}_{\mathrm{BCFY}}(z;r),$$

where the original BCFY FFs are given by

$$D^{(P)}_{\mathrm{BCFY}}(z;r) = N \frac{rz(1-z)^2}{[1-(1-r)z]^6}\Big[6 - 18(1-2r)z + (21-74r+68r^2)z^2 - 2(1-r)(6-19r+18r^2)z^3 + 3(1-r)^2(1-2r+2r^2)z^4\Big],$$

$$D^{(V)}_{\mathrm{BCFY}}(z;r) = 3N \frac{rz(1-z)^2}{[1-(1-r)z]^6}\Big[2 - 2(3-2r)z + 3(3-2r+4r^2)z^2 - 2(1-r)(4-r+2r^2)z^3 + (1-r)^2(3-2r+2r^2)z^4\Big].$$

N is determined analytically from $\int_0^1 dz D^{(P,V)}_{\mathrm{BCFY}}(z;r) = 1$.

$$\tilde{D}^{(V)}_{\mathrm{BCFY}}(z;r) = \theta\left(\frac{m_D}{m_{D^*}} - z\right) D^{(V)}_{\mathrm{BCFY}}\left(\frac{m_{D^*}}{m_D}z;r\right)\frac{m_{D^*}}{m_D}.$$

We fix $m_D = (m_{D^0} + m_{D^\pm})/2 = 1.867$ GeV and $m_{D^*} = (m_{D^{*0}} + m_{D^{*\pm}})/2 = 2.009$ GeV. r is a single nonperturbative parameter.